

Optical properties of graphite

Aleksandra B. Djurišić^{a)} and E. Herbert Li

Department of Electrical and Electronic Engineering, University of Hong Kong, Pokfulam Road, Hong Kong

(Received 3 April 1998; accepted for publication 4 February 1999)

Optical constants of graphite for ordinary and extraordinary waves are modeled with a modified Lorentz–Drude model with frequency-dependent damping. The model enables the shape of the spectral line to vary over a range of broadening functions with similar kernels and different wings, the broadening type being its adjustable parameter. The model parameters are determined by the acceptance-probability-controlled simulated annealing algorithm. Good agreement with the experimental data is obtained in the entire investigated spectral range (0.12–40 eV for ordinary wave and 2.1–40 eV for extraordinary wave). The significant discrepancies between the experimental data obtained by the reflectance measurements and the electron-energy-loss spectroscopy data are analyzed in details. Inconsistency in terms of unsatisfied Kramers–Kronig relations is discovered in the index of refraction data derived from reflectance measurements, and a method for correcting the data is proposed. © 1999 American Institute of Physics.

[S0021-8979(99)02010-1]

I. INTRODUCTION

Graphite is a semimetallic crystalline allotropic form of carbon. Semimetals have even number of valence electrons per unit cell of the crystal, while the presence of free carriers at $T=0$ K is a result of the overlap between the conduction and valence bands. Carbon atoms in monocrystalline graphite are arranged in almost parallel layers. In each layer, carbon atoms form a network of regular hexagons. Since the interplanar distance of the neighboring layers is around 2.7 times greater than that between the two nearest neighboring C atoms in one layer, a large anisotropy in structural, electronic and optical properties exists. The dielectric constant tensor of graphite as a solid with hexagonal lattice symmetry has two independent components: $\epsilon_{\perp} = \epsilon_{1\perp} + i\epsilon_{2\perp}$ and $\epsilon_{\parallel} = \epsilon_{1\parallel} + i\epsilon_{2\parallel}$. They correspond to two different polarization directions of the electric field E . More specifically, $E \perp c$ denotes the ordinary wave and $E \parallel c$ the extraordinary wave, where c is a symmetry axis perpendicular to the basal plane. Since the cleavage plane is perpendicular to the c axis, ϵ_{\perp} can be easily determined by the normal incidence reflectance measurements. At the same time, though, ϵ_{\parallel} cannot be obtained in such a way, mostly because of the difficulties involved in preparing suitable surfaces parallel to the c axis.

The optical properties of graphite have been studied experimentally.^{1–7} Several attempts have been made to identify the optical transitions in the band structure of graphite, which correspond to most of the characteristic features of optical spectra.^{8–11} Some of the measurements have been performed on the natural single crystals.^{1,3,12,13} However, such crystals of graphite are very fragile and usually contain large concentrations of impurities. Some of these impurities may be removed by chemical treatment like prolonged boiling in concentrated hydrofluoric acid or heating to ~ 2000 °C

in flowing fluorine gas, thus leaving ppm levels of metallic impurities such as Fe. Since high-purity natural single crystals are hard to obtain, highly oriented pyrolytic graphite (HOPG) is often used for measurements of the physical properties of graphite. HOPG consists of a large number of crystallites with c axis well aligned (within $\sim 0.2^\circ$ of the average c axis), so its properties are very similar to those of the natural single crystals.¹⁴ It has been shown that the reflectance spectrum of HOPG agrees to within the experimental error with the reflectance spectrum of natural single crystals.^{1,3}

Different techniques have been used to investigate the optical properties of graphite. The data obtained for the ordinary wave show reasonable agreement among themselves. In the case of ϵ_{\parallel} , however, significant disagreement exists among the available sets of experimental data. Ignoring the differences inherent in the techniques used (optical, electron-energy-loss spectroscopy), this disagreement may be caused by the difficulty in obtaining good surfaces parallel to the c axis, and the fact that all optical data are derived from reflectivity measurements. Therefore, scattering among the data can be partially explained by errors connected to Kramers–Kronig analysis of reflectivity at near-normal incidence, the difficulty of obtaining absolute values of reflectivity (particularly for large angles of incidence), and the different surface conditions which can significantly affect the reflectivity. However, these experimental difficulties do not explain why there are significant differences between ϵ_{\parallel} obtained by reflectivity measurements and that by electron-energy-loss spectroscopy (EELS) in the range 2–18 eV. In particular, EELS data give a sharp peak at around 11 eV in $\epsilon_{2\parallel}$, which is several times larger than the estimated experimental uncertainty,² which is absent in the optical data. Also, the band structure calculations predict that there would be a band gap of around 5 eV for the parallel polarization, but this does not coincide with the EELS data. Despite many at-

^{a)}Electronic mail: dalek@pppns1.phy.tu-dresden.de

tempts to correlate the experimental dielectric function features with the transitions predicted by band structure calculations,^{3,5,8,10,11,15-17} the question as to whether EELS data or optical data would describe the optical properties for extraordinary waves in graphite more accurately is still unresolved.

The main purpose of this article is to model the optical constants of graphite over a wide frequency range (0.12–40 eV for ϵ_{\perp} and 2–40 eV for ϵ_{\parallel}). We employ the modified Lorentz–Drude oscillator model. In this model, damping is described with the frequency-dependent function instead of a constant, with one additional parameter per oscillator. In this way, the shape of the spectral line is an adjustable parameter of the model, thus allowing greater flexibility. Since the model is based on damped harmonic oscillators, it satisfies the causality, linearity, reality and Kramers–Kronig requirements. This enables us to assess and discuss the conflicts and disagreements in different sets of experimental data. An inconsistency in the optical constants of graphite for the parallel polarization obtained by optical measurements has been discovered, and a method for correcting the data in agreement with Kramers–Kronig relations is proposed.

The article is organized as follows. Section II presents a detailed description of the model of optical constants employed. In Sec. III, the results obtained are presented, and an analysis of the existing experimental data is given in detail. The EELS and the optical data for the parallel polarization are compared and the proposed method for correcting the optical data is described. Finally, conclusions are drawn.

II. DESCRIPTION OF THE MODEL

We shall briefly describe the model for the optical dielectric function. It has been shown^{18–21} that the dielectric function $\epsilon_r(\omega)$ can be expressed as

$$\epsilon(\omega) = \epsilon^{(f)}(\omega) + \epsilon^{(b)}(\omega), \tag{1}$$

where the intraband effects $\epsilon^{(f)}$ (usually referred to as free-electron effects) are separated from the interband effects $\epsilon^{(b)}$ (usually referred to as bound-electron effects).

The intraband part $\epsilon^{(f)}(\omega)$ of the dielectric function is described by the free-electron or Drude model:²²

$$\epsilon^{(f)}(\omega) = 1 - \frac{\Omega_p^2}{\omega(\omega + i\Gamma_0)}, \tag{2}$$

where $\Omega_p = \sqrt{f_0}\omega_p$ is the plasma frequency associated with intraband transitions with the oscillator strength f_0 and the damping constant Γ_0 .

The interband contribution to the dielectric function $\epsilon^{(b)}(\omega)$ is described by the modified Lorentz model. This model assigns oscillators to major critical points in the joint density of states corresponding to interband transition energies $\hbar\omega_j$, with some additional oscillators modeling the absorption between the critical points. Each oscillator is characterized by its oscillator strength f_j , the damping constant Γ_j and frequency ω_j . The contribution of the interband transitions is given by

$$\epsilon^{(b)}(\omega) = - \sum_{j=1}^k \frac{F_j}{(\omega^2 - \omega_j^2) + i\omega\Gamma_j}, \tag{3}$$

where k is the number of employed oscillators and $F_j = f_j\omega_p^2$.

However, it has already been revealed that Lorentzian broadening does not accurately describe the absorption processes in a solid.^{23–25} One principal reason is that the Lorentzian shape of the spectral line is characterized by wide wings, resulting in higher absorption and higher values of the imaginary part of the dielectric function ϵ_2 . Here, therefore, we introduce a simple modification which allows the absorption lineshape to vary over a range of broadening functions. Kim *et al.*²⁶ have proposed replacing the damping constant Γ_j with the frequency-dependent expression

$$\Gamma'_j = \Gamma_j \exp \left[-\alpha_j \left(\frac{\hbar\omega - \hbar\omega_j}{\Gamma_j} \right)^2 \right]. \tag{4}$$

It has been shown that for suitable values of the parameter α_j , the shape of the imaginary part of the dielectric function can closely mimic the Gaussian one.²⁶ Recently, Rakić and Majewski²⁷ have shown that better agreement with the experimental data for GaAs/AIAs can be obtained by including the above expression in Adachi's model of optical properties of semiconductors.²⁸ Therefore, we employ a similar modification of the Lorentz–Drude model, where Γ_j in each interband transition in Eq. (3) is replaced with the expression given by Eq. (4). When the dielectric function is determined, the real and imaginary parts of the index of refraction $N = n + ik$ are calculated from the expressions:

$$n = \sqrt{1/2(\epsilon_1 + \sqrt{\epsilon_1^2 + \epsilon_2^2})} \tag{5}$$

and

$$k = \sqrt{1/2(-\epsilon_1 + \sqrt{\epsilon_1^2 + \epsilon_2^2})}. \tag{6}$$

The model parameters are determined by minimizing the following objective function:

$$F = \sum_{i=1}^{i=N} \left[\left| \frac{\epsilon_1(\omega_i) - \epsilon_1^{\text{expt}}(\omega_i)}{\epsilon_1^{\text{expt}}(\omega_i)} \right| + \left| \frac{\epsilon_2(\omega_i) - \epsilon_2^{\text{expt}}(\omega_i)}{\epsilon_2^{\text{expt}}(\omega_i)} \right| \right]^2, \tag{7}$$

where $\epsilon_1(\omega_i)$, $\epsilon_2(\omega_i)$ are the calculated values of the real and imaginary parts of the dielectric constant at frequency ω_i ; $\epsilon_1^{\text{expt}}(\omega_i)$ and $\epsilon_2^{\text{expt}}(\omega_i)$ are the corresponding experimental values.

III. RESULTS AND DISCUSSION

For both polarizations, seven oscillators are employed. The model parameters are determined by acceptance-probability-controlled simulated annealing algorithm with the adaptive move-generation procedure.^{29,30} The experimental data used in this work are tabulated in *Handbook of Optical Constants II*.⁶

A. Discussion on the optical constants corresponding to $E_{\perp}c$

For ϵ_{\perp} , the data obtained by Klucker, Skibawski, and Steinmann⁷ are used in the range 5–40 eV, the data from Greenaway *et al.*³ in the range 2–5 eV and the data of Nemanich, Lucowsky, and Solin³¹ in the range 0.12–0.22 eV. Klucker, Skibawski, and Steinmann⁷ measured the reflectivity of freshly cleaved HOPG samples between 3 and 40 eV for different angles of incidence. The synchrotron radiation was polarized either parallel or perpendicular to the plane of incidence with a degree of polarization between 0.9 and 0.97. The relative reflectance measurements for nine angles between 15° and 75° were performed, and ϵ_{\perp} and ϵ_{\parallel} were determined by fitting R with the Fresnel formula for anisotropic uniaxial crystals. Absolute R at 15° (near-normal incidence) was used to obtain ϵ_{\perp} by the Kramers–Kronig analysis. The overall agreement with other optical measurements and with the EELS data is good.

Greenaway *et al.*³ measured the reflectance of both natural single crystals and HOPG. The HOPG samples were prepared by cutting and mechanical polishing without the etching procedure. The surface area had a high degree of flatness, and R_s and R_p (reflectances corresponding to the electric field E perpendicular and parallel to the plane of incidence, respectively) were measured from 1.9 to 5.15 eV at incidence angles from 10° to 80° in steps of 10° and at angles of 75°, 85° and 87°. In addition, R on polished surfaces, both parallel and perpendicular to the c axis, was measured in the 2–9 eV range in order to compare $E_{\perp}c$ and $E_{\parallel}c$ under identical surface conditions. Those data were not suitable for Kramers–Kronig analysis because of the inferior quality of polished surfaces compared with the cleaved ones. The values of n_{\perp} , k_{\perp} and n_{\parallel} , k_{\parallel} from 0.9 to 15.5 eV were obtained by the least-squares fit of R_s and R_p at different angles of incidence with the Fresnel relations for uniaxial materials. The values of n_{\perp} and k_{\perp} are in good agreement ($\pm 10\%$) with the data from Taft and Philipp¹ and the data from Klucker, Skibawski, and Steinmann.⁷

In the infrared region, the data from Nemanich, Lucowsky, and Solin³¹ are employed. They measured the reflectivity of HOPG for $E_{\perp}c$ on the cleaved surfaces and for $E_{\parallel}c$ on the polished surfaces. The surface damage induced by polishing was accounted for by scaling the $E_{\parallel}c$ spectrum with the ratio of $E_{\perp}c$ spectra obtained from the cleaved surface and the polished surface respectively.

Figure 1 shows the real and imaginary parts of the index of refraction corresponding to $E_{\perp}c$ vs energy. The open circles represent the experimental data, while the solid line represents the calculated values obtained for the parameters given in Table I. Good agreement between the experimental and calculated data can be observed for both the real and imaginary parts of the index of refraction. It should be noted that the experimental data for ϵ_{\perp} obtained by the EELS and by the reflectivity measurements agree well among themselves; they also agree well with the theoretical calculations. The experimental data for $\epsilon_{2\perp}$ show a sharp peak at 4.5 eV and a broader peak at around 14.5 eV, which can be accounted for by band structure calculations.^{3,4,8,9,11,15–17}

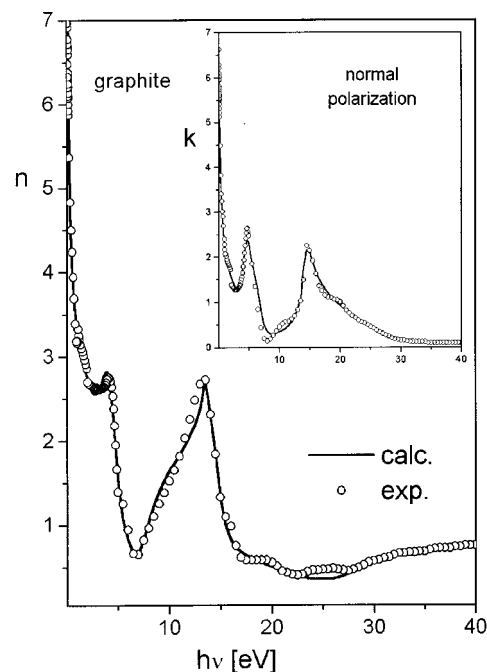


FIG. 1. Real part of the index of refraction n_{\perp} of graphite as a function of energy for normal polarization. The inset shows the imaginary part of the index of refraction k_{\perp} vs energy. The open circles represent experimental data, while the solid line represents calculated values.

Plasma frequency corresponding to collective excitations of π electrons is around 7 eV,^{1,4,5,7,32} while the $\pi + \sigma$ plasmon corresponding to the collective excitation of all four electrons is around 27 eV.^{5,7} This is in contrast with the earlier work of Taft and Philipp,¹ which predicts the $\pi + \sigma$ plasmon to be at around 25 eV. An effective number of electrons per atom, calculated for the experimental data for normal polarization saturates at 4 electrons per atom above 30 eV, as expected (for 1π and 3σ electrons).^{1,5,7}

B. Discussion on the optical constants corresponding to $E_{\parallel}c$

Contrary to the ϵ_{\perp} data, there are significant discrepancies between the EELS and the reflectance data for ϵ_{\parallel} . The theoretical calculations also disagree in certain aspects. Major discrepancies between the EELS and the optical data occur in the range from 2 to 18 eV. Beyond 18 eV, the EELS data by Venghaus² join smoothly with the reflectance data of Klucker, Skibawski, and Steinmann.⁷ Venghaus measured electron-energy-loss spectrum of HOPG samples at about 1000 Å thickness. The resulting ϵ_{\parallel} was in very good agreement with the previous EELS measurements. A sharp maximum in $\epsilon_{2\parallel}$, which is absent in the optical data, was established beyond experimental and computational errors. Band structure calculations also disagree among themselves over this point, giving no conclusive evidence in favor of or against the strong transition at ~ 11 eV. The existence of a peak around 11 eV is in agreement with the calculations of Bassani and Parravicini.¹⁶ The calculations of Painter and Ellis,¹¹ though, predict the existence of transitions at 13.5 eV or even at 16 eV, and calculations of Tossati and Bassani⁵ predict transitions to be at around 11 and 16 eV.

TABLE I. Final values for modified LD model parameters, Γ_j, ω_j (eV), f_j, α_j dimensionless, $j=1,7$. The oscillator-strength values correspond to plasma frequencies 27 eV for normal polarization and 19 eV for parallel polarization.

Material	$E \perp c$	$E \parallel c$, EELS	$E \parallel c$, optical
ϵ_∞	1.070	1.108	0.731
f_0	0.014	0.016	—
Γ_0	6.365	0.091	—
f_1	0.073	0.134	0.034
Γ_1	4.102	9.806	2.096
ω_1	0.275	2.358	11.418
α_1	0.505	24.708	0.138
f_2	0.056	0.072	0.003
Γ_2	7.328	4.727×10^2	3.492
ω_2	3.508	5.149	4.095
α_2	7.079	0.524	29.728
f_3	0.069	0.307	0.078
Γ_3	1.414	4.651	2.442
ω_3	4.451	13.785	10.003
α_3	0.362	0.217	0.516
f_4	0.005	0.380	0.131
Γ_4	0.046	1.797	2.529
ω_4	13.591	10.947	14.991
α_4	7.426	0.518	1.78×10^{-6}
f_5	0.262	0.065	0.280
Γ_5	1.862	2.418	6.829
ω_5	14.226	16.988	17.516
α_5	3.82×10^{-4}	0.286	$1.01.78 \times 10^{-6}$
f_6	0.460	0.553	0.855
Γ_6	11.922	21.395	14.541
ω_6	15.550	24.038	30.712
α_6	1.387	0.248	1.180
f_7	0.200	1.381	0.972
Γ_7	39.091	37.025	20.314
ω_7	32.011	36.252	46.004
α_7	28.963	15.101	9.388

Serious disagreement also exists in the range below 6 eV. Data from Greenaway *et al.*³ and from Ergun¹³ show no structure in this region, which is in agreement with the band structure calculations employing a two-dimensional approximation.^{5,16} However, the calculations of Johnson and Dresselhaus⁸ predict a peak near 4.3 eV, which is also present in the data from Klucker, Skibawski, and Steinmann.⁷ A possible reason for the absence of this small peak in former cases can be the slight depolarization of light in their experiments. Transitions between π bands, which are forbidden for $E \parallel c$ in a single layer, are not strictly forbidden in a three-dimensional lattice. Nevertheless, the matrix elements are much smaller than those for the perpendicular polarization, thus accounting for the small magnitude of the peak.^{8,10} However, the breakdown of the selection rules for the three-dimensional case predicted by calculations of Johnson and Dresselhaus⁸ still does not justify data obtained by the EELS in this region.

It is difficult to establish which of those two methods, the reflectance measurements or the EELS, is correct. Reflectance measurements of the optical constants for $E \parallel c$ cannot be performed directly because of the difficulties in preparing suitable good quality surfaces. Therefore, values of the index of refraction for the parallel polarization have to be deduced from reflectance measurements at oblique incidence. For an anisotropic material, at each wavelength a function of five variables (the real and imaginary parts of the dielectric func-

tion for perpendicular polarization, the real and imaginary parts of the dielectric function for parallel polarization and the degree of polarization) is minimized in order to determine values which give minimal discrepancy between calculated and measured reflectances. It is well known that this is not a simple problem (mainly due to the existence of multiple solutions), even in a simple case of isotropic material and reflectance measurements at normal incidence, where only two variables, n and k , have to be determined. Hence, there exists a large uncertainty of the determined values ($\pm 10\%$). On the other hand, the EELS may not be accurate in the low-energy range, because in this range, the relativistic (Cherenkov) effects contribute significantly to the energy loss when the momentum transfer has large components along the c axis.⁵ Another strong objection to the EELS data is that they do not agree with theoretical prediction of the band gap of about 5 eV. In order to check the consistency of the experimental data, finite-energy sum rules have been applied in the literature.^{5,7} However, the effective number of electrons per atom in case of parallel polarization, as calculated from both the EELS data⁵ and reflectance data,⁷ is below three at 40 eV (and it is far from saturation since plots show slope of about 45°), so that no conclusion can be drawn from that except that there are some higher-lying transitions involving the valence-band electrons.

Since all previous theoretical considerations (for recent first-principles calculations, see Ref. 10) have failed to resolve the issue as to whether the EELS or the optical data represent an accurate description of the optical constants of graphite for the parallel polarization, we have tried to model both sets of available data for ϵ_{\parallel} . The first set consists of the EELS data by Venghaus in the 2–18 eV range and the data of Klucker, Skibawski, and Steinmann⁷ in the range from 18 to 40 eV. The second set consists of the data derived from the reflectance measurements of Greenaway *et al.*³ in the 2–5 eV range and the data of Klucker, Skibawski, and Steinmann⁷ in the range 5–40 eV. Plasma frequencies for ϵ_{\parallel} are at around 14 eV⁵ and around 19 eV.^{5,7} Figure 2 shows the real and imaginary parts of the index of refraction corresponding to $E \parallel c$ as a function of energy. The open circles represent the EELS experimental data, while the solid line represents the calculated values obtained for the parameters given in Table I. A very good agreement between experimental and calculated values can be observed.

As mentioned earlier, the optical data show existence of a band gap predicted by theoretical calculations. Therefore, in modeling the optical data we do not consider the intraband contributions because they would not be consistent with the small values of k_{\parallel} for low energies. However, in trying to fit the set of data derived from the reflectance measurements, we encountered unexpected difficulties. When we attempted to adopt the usual objective function [given by Eq. (7)] which minimizes discrepancies between experimental and calculated data for both the real and imaginary parts of the dielectric function, or the index of refraction, the algorithm did not converge at all. Changing the number of oscillators employed did not appear to influence this. Since we are employing a global optimization routine, which has been severely tested for problems with up to 100 variables and up to

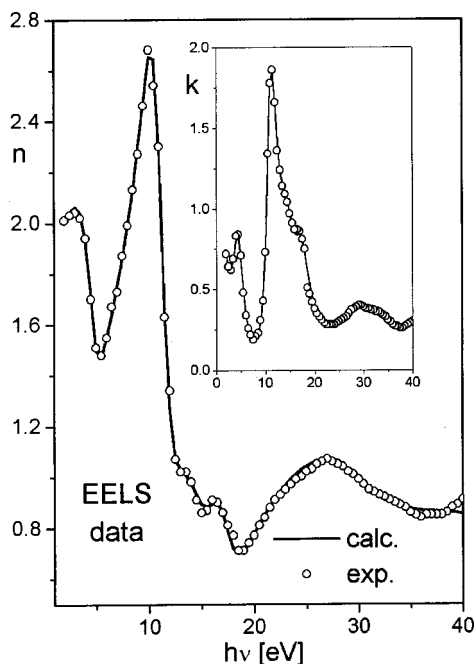


FIG. 2. Real part of the index of refraction $n_{||}$ of graphite as a function of energy for normal polarization. The inset shows the imaginary part of the index of refraction $k_{||}$ vs energy. The open circles represent EELS experimental data, while the solid line represents calculated values.

15^{100} local minima,³⁰ the only reason for divergence could be that the experimental data cannot be described with the model employed. On the other hand, there is no reason why the optical constants of any material in the investigated spectral range could not be described with the Lorentz or Lorentz–Drude oscillator model. Then, we tried to fit separately the real and imaginary parts of the refractive index, and the results are shown on Figs. 3 and 4, respectively. In minimizing the squared relative errors for n and k separately, no numerical problems were encountered. However, it turned

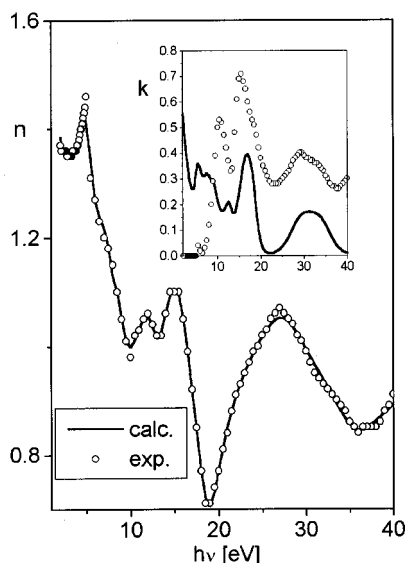


FIG. 3. Refractive index $n_{||}$ as a function of energy. The open circles represent experimental data from optical measurements, while the solid line represents calculated values. The inset shows $k_{||}$ as a function of energy.

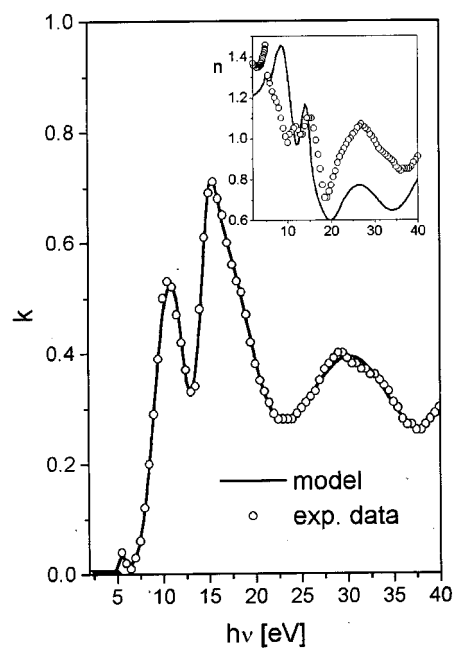


FIG. 4. Coefficient of extinction $k_{||}$ vs energy. The open circles represent experimental data from optical measurements, while the solid line represents calculated values. The inset shows $n_{||}$ as a function of energy.

out that excellent agreement for the real part of the index of refraction $n_{||}$, as shown on Fig. 3, leads to poor agreement for the imaginary part $k_{||}$, and *vice versa*, as shown on Fig. 4. Since the model automatically satisfies Kramers–Kronig relations, the agreement with the experimental data should be, in principle, equally good for both the real and imaginary parts of the index of refraction. Moreover, it can be observed that the refractive index experimental curve fails to show a structure corresponding to the obvious peak in the coefficient of extinction around 11 eV. Also, there is no justification for a very sharp peak in experimental $n(\omega)$ near 5 eV, which appears to be totally unrelated to any feature of $k(\omega)$. It should be pointed out that values for the real and imaginary parts of the dielectric function for the parallel polarization were calculated independently at each wavelength,⁷ so that there is no guarantee that the experimental data satisfy Kramers–Kronig relations. Therefore, we have decided to check whether the experimental data are Kramers–Kronig consistent.

We have performed Kramers–Kronig transformation for the set of data for the imaginary part of the index of refraction $k_{||}$. Since the data of Klucker, Skibawski, and Steinmann⁷ cover 3–40 eV range, we have used the data of Greenaway *et al.*³ from 2 to 3 eV. In the region where these two data sets overlap, we have chosen to use the data of Klucker, Skibawski, and Steinmann⁷ because these data show a weak peak in $k_{||}$, as predicted by the band-structure calculations based on three-dimensional approximation.⁸ The data for the imaginary part of the index of refraction resemble theoretically predicted structure. There is one small peak at around 4.3 eV, which is due to the breakdown of selection rules for three-dimensional lattice,⁸ and a two peak structure at around 11 and 14 eV.¹⁰ Obtained results are de-

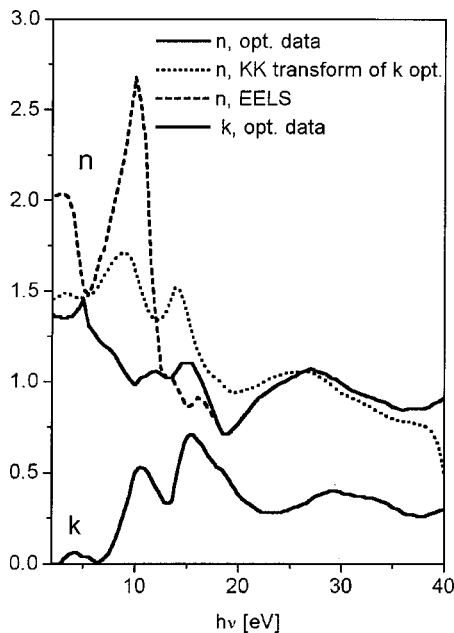


FIG. 5. Comparison among the available sets of data for n_{\parallel} —tabulated experimental data from the optical measurements (solid line), the result of Kramers–Kronig transformation (dotted line), and data obtained by the EELS (dashed line).

picted in Fig. 5, showing the comparison between the tabulated experimental data (solid line) and the result of Kramers–Kronig transformation (dotted line). Data obtained by the EELS are represented by the dashed line. It can be observed that Kramers–Kronig transformation gives curve for n_{\parallel} which significantly differs from the tabulated data, where only differences at the end of range can be attributed to the errors in the Kramers–Kronig analysis. Those errors are in part due to the higher-lying transitions whose existence can be deduced from the fact that the effective number of electrons per atom for the parallel polarization is far from saturation value at 40 eV.^{5,7} Since the real and imaginary parts of the index of refraction have to satisfy Kramers–Kronig relations, we have decided to model the original experimental data given for k_{\parallel} , while for n_{\parallel} , we employ the Kramers–Kronig transformation of experimental values of k_{\parallel} in the spectral range up to around 26 eV, and the original experimental values of n_{\parallel} from 26 to 40 eV to avoid errors induced by the Kramers–Kronig transformation at the end of the region. Figure 6 shows the real and imaginary parts of the index of refraction as a function of energy. The open circles represent the experimental data for the imaginary part, the triangles represent the real part obtained by Kramers–Kronig transformation, while the solid line represents the calculated values obtained for the parameters given in Table I. It can be observed that for this composite set of data (original experimental values for k_{\parallel} and Kramers–Kronig transformation for n_{\parallel}), there exists good agreement with the experiment for both the real and imaginary parts of the index of refraction.

Therefore, to describe the optical constants of graphite for the parallel polarization, one should use the data obtained from optical measurements for the imaginary part of the index of refraction, while for the real part, the Kramers–

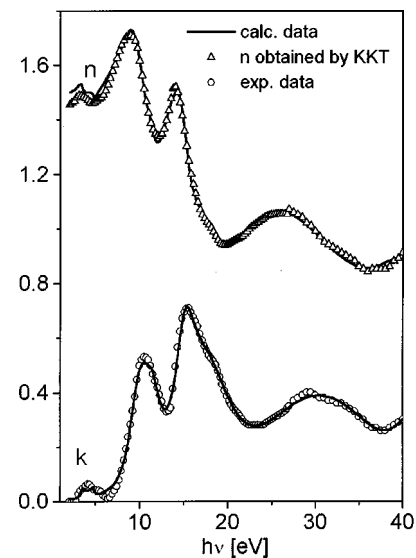


FIG. 6. Real and imaginary parts of the index of refraction of graphite vs energy for parallel polarization. Open circles represent the experimental data for the imaginary part of the index of refraction, while triangles represent the real part obtained by Kramers–Kronig transformation and the solid line represents calculated results.

Kronig transformation of these data should be employed. The data set obtained in such a manner, which can be easily and accurately reproduced by the model described here, is internally consistent and in agreement with the theoretically predicted optical transitions. Based on the band-structure calculations, there is reasonable doubt concerning the accuracy of the EELS data for lower energies, especially when the EELS data do not confirm the existence of a gap of about 5 eV for parallel polarization. While Tossati and Bassani⁵ have pointed out that the EELS technique for low energies could be inaccurate, other authors who have performed EELS measurements do not question its adequacy. With no conclusive evidence in support of our disregarding the EELS set of data altogether, we have decided to model both the EELS and the optical data set. Yet, based on band-structure calculations, we believe that the data obtained from optical measurements should be more accurate. In any case, further experimental efforts to resolve this problem are highly desired.

IV. CONCLUSION

The optical properties of graphite are modeled using the modified Lorentz–Drude model with frequency-dependent damping for the perpendicular polarization in the 0.12–40 eV range, and for the parallel polarization in the 2–40 eV range. The significant discrepancies among various sources of experimental data for ϵ_{\parallel} are investigated. In light of the existing band-structure calculations, there is reasonable doubt in the accuracy of the EELS data for parallel polarization. There also exists serious inconsistency in the tabulated values of the real and imaginary parts of the index of refraction obtained by optical measurements. The tabulated values of n_{\parallel} do not represent Kramers–Kronig transformation of k_{\parallel} , and *vice versa*. Therefore, to model the optical properties of graphite for extraordinary waves, we have to derive a consistent set of experimental data. For the set of data for k_{\parallel}

obtained from optical measurements in such a manner that they are in agreement with band-structure calculations (i.e., using data of Klucker, Skibawski, and Steinmann in the range 3–5 eV which show a weak peak at around 4.3 eV), Kramers–Kronig transformation is performed to determine n_{\parallel} . By doing so, we have obtained the set of data which satisfies Kramers–Kronig relations and agrees with the band-structure calculations. The values of n_{\parallel} thus obtained should be used, instead of the originally given experimental values. Using our model's parameter values, the set of data derived in the described manner and the EELS set of data can be accurately reproduced.

ACKNOWLEDGMENTS

This work is supported by the Research Grant Council (RGC) Earmarked Grant of Hong Kong. One of the authors (A.B.D.) would also like to acknowledge the support of William Mong Postdoctoral fellowship for this work.

¹E. Taft and H. R. Philipp, Phys. Rev. A **138**, 197 (1965).

²H. Venghaus, Phys. Status Solidi B **71**, 615 (1975).

³D. L. Greenaway, G. Harbeke, F. Bassani, and E. Tossati, Phys. Rev. **178**, 1340 (1969).

⁴G. Guizzetti, L. Nosnezo, E. Reguzzoni, and G. Samoggia, Phys. Rev. Lett. **31**, 154 (1973).

⁵E. Tossati and F. Bassani, Nuovo Cimento B **65**, 161 (1970).

⁶A. Borghesi and G. Guizzetti, in *Handbook of Optical Constants of Solids II*, edited by E. D. Palik (Academic, Boston, 1991), pp. 449–460.

⁷R. Klucker, M. Skibowski, and W. Steinmann, Phys. Status Solidi B **65**, 703 (1974).

⁸L. G. Johnson and G. Dresselhaus, Phys. Rev. B **7**, 2275 (1973).

⁹R. F. Willis, B. Fitton, and G. S. Painter, Phys. Rev. B **9**, 1926 (1973).

¹⁰R. Ahuja, S. Auluck, J. M. Wills, M. Alouani, R. Johansen, and O. Eriksson, Phys. Rev. B **55**, 4999 (1997).

¹¹G. S. Painter and D. E. Ellis, Phys. Rev. B **1**, 4747 (1970).

¹²W. B. Boyle and P. Nozieres, Phys. Rev. **111**, 782 (1958).

¹³S. Ergun, Nature (London) **211**, 135 (1967).

¹⁴*Chemistry and Physics of Carbon*, edited by P. L. Walker, Jr. and P. A. Thrower (Marcel Dekkers-Kroniger Inc., New York, 1965), Vol. 16, pp. 138–161.

¹⁵N. B. Bonnet, S. M. Chudinov, and Ya. G. Ponomarev, in *Semimetals I: Graphite and its Compounds; Modern Problems in Condensed Matter Sciences, Vol. 20.1* series editors, edited by V. M. Agranovich and A. A. Maradudin (North-Holland, Amsterdam, 1988).

¹⁶F. Bassani and G. Pastori Parravicini, Nuovo Cimento B **VL**, 85 (1967).

¹⁷E. Doni and G. Pastori Parravicini, Nuovo Cimento B **64**, 117 (1969).

¹⁸N. W. Ashcroft and K. Sturm, Phys. Rev. B **3**, 1898 (1971).

¹⁹H. Ehrenreich, H. R. Philipp, and B. Segall, Phys. Rev. **132**, 1918 (1963).

²⁰H. Ehrenreich and H. R. Philipp, Phys. Rev. **128**, 1622 (1962).

²¹K. Sturm and N. W. Ashcroft, Phys. Rev. B **10**, 1343 (1974).

²²M. I. Marković and A. D. Rakić, Appl. Opt. **29**, 3479 (1990).

²³O. Stenzel, R. Petrich, W. Scharff, A. Tikhonravov, and V. Hopfe, Thin Solid Films **207**, 324 (1992).

²⁴A. Franke, A. Stendal, O. Stenzel, and C. von Borczyskowski, Pure Appl. Opt. **5**, 845 (1996).

²⁵R. Brendel and D. Borman, J. Appl. Phys. **71**, 1 (1992).

²⁶C. C. Kim, J. W. Garland, H. Abad, and P. M. Raccach, Phys. Rev. B **45**, 11749 (1992).

²⁷A. D. Rakić and M. L. Majewski, J. Appl. Phys. **80**, 5509 (1996).

²⁸S. Ozaki and S. Adachi, J. Appl. Phys. **78**, 3380 (1995).

²⁹A. D. Rakić, J. M. Elazar, and A. B. Djurišić, Phys. Rev. E **52**, 6862 (1995).

³⁰A. B. Djurišić, A. B. Rakić, and J. M. Elazar, Phys. Rev. E **55**, 4797 (1997).

³¹R. J. Nemanich, G. Lucowsky, and S. A. Solin, Solid State Commun. **23**, 117 (1977).

³²J. G. Carter, R. H. Huebner, R. W. Hamm, and R. D. Birkhoff, Phys. Rev. A **137**, A635 (1965).